Fluctuation Theorem Applied to F_1-ATPase

Kumiko Hayashi, Hiroshi Ueno, Ryota Iino, and Hiroyuki Noji*

The Institute of Scientific and Industrial Research, Osaka University, 8-1 Mihogaoka, Ibaraki 567-0047, Osaka, Japan

(Received 18 February 2010; published 28 May 2010)

In recent years, theories of nonequilibrium statistical mechanics such as the fluctuation theorem (FT) and the Jarzynski equality have been experimentally applied to micro and nanosized systems. However, so far, these theories are seldom applied to autonomous systems such as motor proteins. In particular, representing the property of entropy production in a small system driven out of equilibrium, FT seems suitable to be applied to them. Hence, for the first time, we employed FT in the single molecule experiments of the motor protein F_1-adenosine triphosphatase (F_1), in which the rotor γ subunit rotates in the stator $\alpha_3\beta_3$ ring upon adenosine triphosphate hydrolysis. We found that FT provided the better estimation of the rotary torque of F_1 than the conventional method.

DOI: 10.1103/PhysRevLett.104.218103 PACS numbers: 87.15.Ya, 05.40.−a

Experimental applications of the fluctuation theories of nonequilibrium statistical mechanics [1–4] to micro and nanosized systems have been conducted with technical development in both the manipulation and observation of objects on small scales [5–12]. Particularly, the fluctuation theorem (FT), which represents the property of entropy production in a small nonequilibrium system, has been applied to various physical systems such as colloidal particle systems, granular systems, and turbulent systems [5–8].

The theories of nonequilibrium statistical mechanics have recently been actively applied to biological systems [8–12]. As to FT, the work fluctuation theorem was investigated in RNA hairpin systems [10]. Unlike RNA hairpins, motor proteins autonomously move by using the free energy of chemical reactions. Can FT be verified for such an autonomously nonequilibrium system? Which expression of FT is useful in elucidating the thermodynamic properties of motor proteins? To answer these questions, we extend the applicability of FT to the single molecule experiment of F_1-adenosine triphosphatase (ATPase) (F_1), in which the γ subunit rotates in the $\alpha_3\beta_3$ ring with adenosine triphosphate (ATP) hydrolysis. We focus on its rotary torque measurement, and propose FT as a new tool for nonequilibrium force measurement of a wide range of biological systems *in vitro* and *in vivo*.

Single molecule experiment.—F_1 is a rotary motor protein and a part of F_oF_1-ATPase/synthase [13–20]. The minimum complex acting as a motor is the $\alpha_3\beta_3\gamma$ subcomplex, and the γ subunit rotates in the $\alpha_3\beta_3$ ring upon ATP hydrolysis [13]. The three catalytic β subunits hydrolyze ATP sequentially and cooperatively. Three ATP molecules are hydrolyzed per turn, or in other words, the free energy obtained from single ATP hydrolysis is used for a 120° rotation [14]. The conformations of the β subunits change as the elementary chemical steps such as the ATP binding, the ATP hydrolysis (cleavage of the covalent bond) and the product [adenosine diphosphate (ADP) and inorganic phosphate] releases proceed [Fig. 1(a)], and the coordinated push-pull motion of the C-terminal domains of the β subunits produces torque for the γ subunit to rotate [15,16].

In our single molecule assay (see *Methods*), the rotation of the γ subunit was observed as the rotation of a probe attached to it [Fig. 1(b)] because the size of the γ subunit (~2 nm) is too small for its rotation to be observed directly under an optical microscope. The rotational angle, $\theta(t)$,

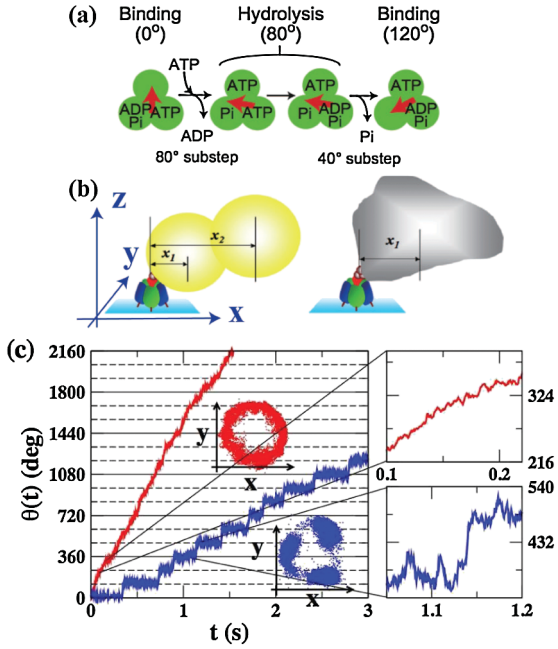

FIG. 1 (color). (a) Reaction scheme of F_1. The green circles and the red arrow represent the β subunits and γ subunit of F_1, respectively. F_1 performs a 120° step rotation upon ATP hydrolysis comprising 80° and 40° substeps. (b) Schematic diagrams of our experimental system (not to scale). The rotation of F_1 is probed by a duplex of polystyrene beads (left) or an irregularly shaped magnetic bead (right). The size of F_1 is about 10 nm and that of a probe is in the range of 358–940 nm. (c) ATP-driven rotations of F_1 probed by the magnetic beads at 1 mM ATP (red line) and 100 nM ATP (blue line).

was calculated from the recorded images of the probe. In Fig. 1(c), $\theta(t)$ is plotted in the cases of 1 mM ATP and 100 nM ATP. While the rotation was continuous for 1 mM ATP, it became stepwise for 100 nM ATP pausing every 120°. The ATP binding dwell (the time that a catalytic site waits for ATP binding) is very short at high [ATP] (<0.1 ms at 1 mM [17]) and the time constant of the dwells for the ATP hydrolysis and that for the product releases are also short (about 1 ms independent of [ATP] for the wild-type F_1 [17]), and a rotation appears continuous when the response time of a probe is longer than these time scales.

In previous studies [14,17–19] assuming that a rotary torque, N, acting on a probe attached to F_1 is constant, N was estimated using the equation

$$N = \Gamma\omega, \tag{1}$$

where ω and Γ are the mean angular velocity and frictional drag coefficient of a rotary probe, respectively. From the calculation of fluid mechanics, the functional forms of Γ for several probes are known as

$$\begin{aligned} \Gamma_{\mathrm{ac}} &= \frac{4\pi\eta L^3}{3[\ln(L/2r)-0.447]} && \text{for an actin filament,} \\ \Gamma_{\mathrm{sb}} &= 8\pi\eta a^3 + 6\pi\eta a x_1^2 && \text{for an a single bead,} \\ \Gamma_{\mathrm{db}} &= 16\pi\eta a^3 + 6\pi\eta a x_1^2 + 6\pi\eta a x_2^2 && \text{for a duplex of beads,} \end{aligned} \tag{2}$$

where L and r are the length and radius of an actin filament, a and x_i ($i = 1, 2$) are the radius and rotation radius of each bead [Fig. 1(b)], and η is the viscosity of a medium ($\eta = 0.89 \times 10^{-9}$ pN s/nm^2 at 25 °C). For the continuous rotation of the wild-type F_1 probed by the actin filament ($L = 2$ μm) at 2 mM ATP, N was estimated to be about 40 pN nm [18].

Although the estimation of the rotary torque of F_1 using Eqs. (1) and (2) seems successful, a problem related to the estimation of Γ remains [20]. When a probe rotates near a glass surface, the real value of Γ is expected to be larger than the value estimated by Eq. (2), which is derived from the assumption that a rotation occurs in a bulk [14,19,20]. In fact, when the probe rotated near the glass surface (~10 nm) [19], the torque has been estimated to be lower than that measured when it rotated away from the glass surface (~200 nm) [14,18]. Noting that this difficulty in estimating Γ is a common problem for force measurements of biological motors such as bacterial flagella [21] and RNA polymerase [22] which move near the surfaces of a cell and a glass, we employ an expression of FT that can estimate N without using the value of Γ to overcome the problem.

Fluctuation theorem.—For a continuous rotation of F_1, the time evolution of $\theta(t)$ is assumed to be described by a Langevin equation

$$\Gamma\frac{d\theta}{dt} = N + \xi(t), \qquad \langle\xi(t)\xi(t')\rangle = 2\Gamma k_B T\delta(t-t'), \tag{3}$$

where ξ is a random force that represents the effect of thermal noise, k_B is the Boltzmann constant, and T is the room temperature ($T = 25$ °C). We also assume that N is constant as was suggested in previous studies [14,17–19]. On the basis of the above model, FT for the torque measurement is expressed as

$$\ln[P(\Delta\theta)/P(-\Delta\theta)] = N\Delta\theta/k_B T, \tag{4}$$

where $\Delta\theta = \theta(t+\Delta t) - \theta(t)$ and $P(\Delta\theta)$ is the probability distribution of $\Delta\theta$.

Verification.—In the following, the torque determined using Eqs. (1) and (2) and that determined using Eq. (4) are denoted as N_Γ and N_{FT}, respectively. Their averaged values are given in Table I (see supplementary material [23] for those of each molecule). Below, we used irregular-shaped magnetic beads (see *Methods*) and duplexes of spherical beads as a probe, which were suitable to observe the rotation of F_1 because of their anisotropic shapes.

For the continuous rotation of the particular F_1 probed by the magnetic bead, $P(\Delta\theta)$ and $\ln[P(\Delta\theta)/P(-\Delta\theta)]$ are plotted for the cases $\Delta t = 2.5$–10 ms in Fig. 2(a). The slopes of the graphs in Fig. 2(a) (Right) are almost the same for all cases $\Delta t = 2.5$–10 ms, and the value of the slopes corresponds to N_{FT} according to Eq. (4). In Table I (a), N_Γ is compared with N_{FT}. Although the magnetic beads have a broad distribution in size (200–700 nm) and are not spherical, their approximate sizes were estimated from the recorded images. We then estimated the values of Γ_{sb} using these approximate sizes assuming that the beads were spherical. The fact $N_{\mathrm{FT}} \sim 40$ pN nm $> N_\Gamma$ implies the effect of the glass surface on the estimation of Γ_{sb}.

TABLE I. (a) Torque estimated using the different methods. (b) Summary of N_{FT} (pN nm) (magnetic bead). Note that n represents the number of molecules investigated.

(a)	probe	N_Γ (pN nm)	N_{FT} (pN nm)
	magnetic bead, $n = 6$	$28 \pm 5.9^{a,e}$	$35 \pm 2.8^{a,c,e}$
	duplex (340 nm), $n = 6$	$23 \pm 3.8^{a,e}$	$38 \pm 2.5^{a,c,e}$
	duplex (470 nm), $n = 4$	$31 \pm 3.3^{a,e}$	$31 \pm 2.6^{a,c,e}$
	duplex (179 nm), $n = 3$	$19 \pm 1.8^{b,e}$	$26 \pm 1.2^{b,c,e}$

(b)	F_1 (wild-type)	F_1 (wild-type)	F_1 (βE190D)	V_1
	$n = 6$	$n = 2$	$n = 3$	$n = 5$
	$35 \pm 2.8^{a,c,e}$	$38 \pm 2.7^{a,d,f}$	$37 \pm 2.4^{a,d,f}$	$33 \pm 2.2^{a,d,f}$

[a]The recording rate was 2000 fps.
[b]The recording rate was 1000 fps.
[c]N_{FT} was estimated in the case $\Delta t = 10$ ms.
[d]N_{FT} was estimated in the case $\Delta t = 2.5$ ms.
[e]Continuous rotation.
[f]Stepping rotation.

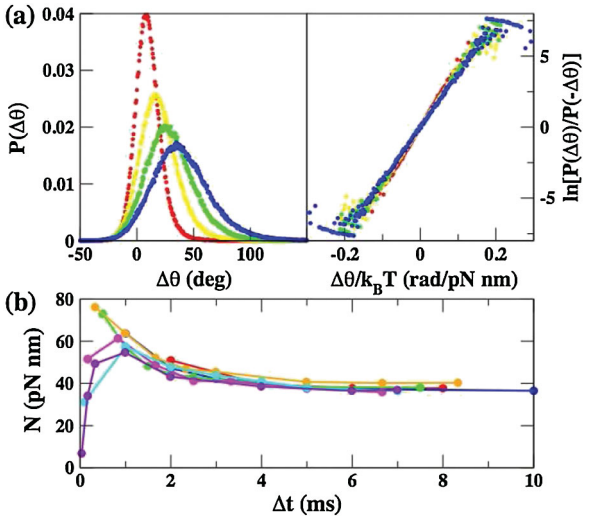

FIG. 2 (color). (a) Probability distribution, $P(\Delta\theta)$, for the cases $\Delta t = 2.5$ ms (red line), 5.0 ms (yellow line), 7.5 ms (green line), and 10 ms (blue line) for the particular F_1 probed by the magnetic bead (left). $\ln[P(\Delta\theta)/P(-\Delta\theta)]$ as a function of $\Delta\theta/k_BT$ (right). The slope was 38 pN nm in the case $\Delta t =$ 10 ms. The recording rate was 2000 fps. (b) N_{FT} as a function of Δt for the recording rates, 500 fps (red line), 1000 fps (blue line), 2000 fps (green line), 3000 fps (orange line), 6000 fps (pink line), 10 000 fps (aqua line), and 30 000 fps (violet line). Here, we used the same molecule probed by the same magnetic bead at 1 mM ATP.

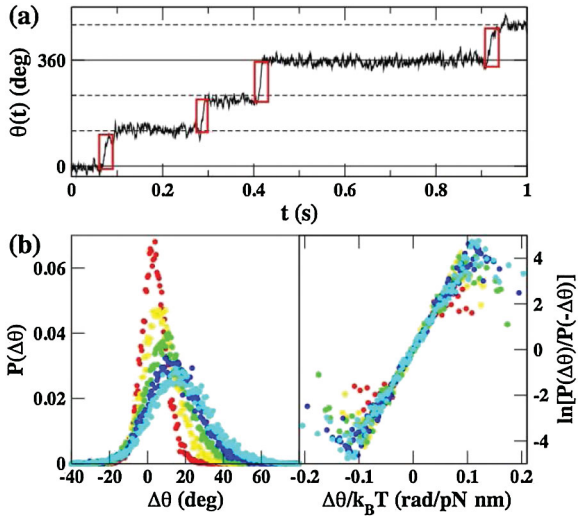

FIG. 3 (color). (a) ATP-driven rotation of F_1 at 100 nM ATP. We analyzed $\theta(t)$ encircled in red (about 100–300 steps). The steps were determined by eye. (b) Probability distributions, $P(\Delta\theta)$, for the cases $\Delta t = 0.5$ ms (red line), 1.0 ms (yellow line), 1.5 ms (green line), and 2.0 ms (blue line), and 2.5 ms (aqua line) for the particular F_1 probed by the magnetic bead (left). $\ln[P(\Delta\theta)/P(-\Delta\theta)]$ as a function of $\Delta\theta/k_BT$ (right). The slope was 40 pN nm in the case $\Delta t = 2.5$ ms. The recording rate was 2000 fps.

To compare N_{FT} and N_Γ more precisely, we used the duplexes of spherical beads [14,17]. When Γ_{db} was used for a duplex, we set $x_1 = 0$ and $x_2 = 2a$ assuming that the duplex typically attached to F_1 perpendicularly to the rotational direction because it is difficult to know precisely how a probe attaches to F_1 using an optical microscope [17]. In the case of the duplex of 340 nm polystyrene beads ($2a = 340$ nm), which are similar in size to the magnetic beads, we again found that $N_{FT} \sim 40$ pN nm $> N_\Gamma$ [Table I (a)].

We also investigated a larger probe (the duplex of 470 nm polystyrene beads), the most part of which is considered to rotate far from a glass surface, and a smaller probe (the duplex of 179 nm polystyrene beads), whose response time is considered to be close to the time constant of the ATP hydrolysis dwell of the wild-type F_1 [17]. In the former case, as expected, it was found $N_{FT} = N_\Gamma$ within statistical error bar [Table I (a)]. Both N_{FT} and N_Γ were slightly smaller than 40 pN nm because the rotary torque may show the load dependence resulted from the intrinsic behavior of F_1 although we cannot exclude the possibility that the torque was lower for this large probe because it may scratch the glass surface during its rotation. In the latter case, both N_{FT} and N_Γ were much smaller than 40 pN nm although $N_{FT} > N_\Gamma$ [Table I (a)] because the existence of the dwells much affected on the fluctuation of the probe, and invalidated the use of Eqs. (1) and (3).

Dependence on the recording rate and Δt.—In our single molecule assays, the average rate of a continuous rotation for the wild-type F_1 depends on the size of a probe and is in the range of 3–40 Hz (see [23] for the rotation rate of each probe). Since we needed to accurately measure the forward and backward fluctuation in $\theta(t)$ to calculate the left-hand side of Eq. (4), the images of the rotating probes were recorded with a high-speed camera [24] at various recording rates [500–30 000 frames per second (fps)] each of which was much higher than the rotation rate. In Fig. 2(b) using the same molecule, N_{FT} is plotted as a function of Δt for the different recording rates. It is seen that for large Δt, N_{FT} converges to almost the same value for all recording rates. Note that below 500 fps, the negative values of $\Delta\theta$, which are needed for the calculation of the left-hand side of Eq. (4), were hardly measured, and reliable estimation of $P(\Delta\theta)/P(-\Delta\theta)$ was difficult. For

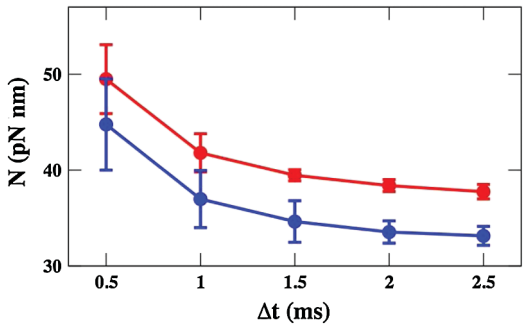

FIG. 4 (color). N_{FT} as a function of Δt for F_1 (red line, 5 molecules) and V_1 (blue line, 5 molecules). The rotations were probed by magnetic beads and recorded at 2000 fps.

small Δt, our numerical simulations suggested that the behavior of N_{FT} might reflect the slight distortion of the rotary potential of F_1 (see [23]).

Application I: Stepping rotations of wild-type F_1 at low [ATP] and mutant F_1 (βE190D).—For the wild-type F_1, the rotation became stepwise at 100 nM ATP. In this case, $\Delta\theta$ was calculated using the 120° steps encircled in red [Fig. 3(a)], assuming that the time evolution of $\theta(t)$ during 120° steps is also described by Eq. (3). In Fig. 3(b), $P(\Delta\theta)$ and $\ln[P(\Delta\theta)/P(-\Delta\theta)]$ are plotted for the cases $\Delta t =$ 0.5–2.5 ms. These values of Δt are smaller than those used at 1 mM ATP because $P(\Delta\theta)$ for Δt larger than 2.5 ms were hard to be measured precisely for the stepping rotation due to a small number of samples.

Next, the mutant $F_1(\beta$E190D) was investigated. Because the glutamic acid at 190 of the β subunit (E190) acts as a general base in the catalysis of ATP hydrolysis, when this residue is mutated into aspartic acid, ATP hydrolysis at the catalytic site is greatly decelerated and $F_1(\beta$E190D) shows 120° stepping even at 1 mM ATP [25]. The fact seen in Table I (b) that the torque was almost the same for the wild type and mutant within statistical error bar implies that the torque caused by the global structural change of the β subunit was not affected greatly by the local mutation while the time constant of ATP hydrolysis was greatly affected. (Note that the torque of the mutant has not been reported previously.)

Application II: V_1-ATPase.—We applied FT (4) to another rotary motor V_1, which is a part of V_oV_1-ATPase [26]. In V_1, the D subunit rotates in the A_3B_3 ring, and 120° steps are observed at low [ATP] (in our case [ATP] = 10 μM). Using Eqs. (1) and (2), the rotary torque of V_1 has been reported to be smaller than that of F_1 [26]. In Fig. 4, it is seen that N_{FT} of V_1 was smaller than that of F_1. This tendency was similar to that observed in the previous study [26].

Summary.—Our results are summarized in Table I (b). Investigating the rotations of F_1 probed by the several kinds of beads and comparing our results with those in Ref. [18], we checked the validity of Eqs. (3) and (4) and found that N_{FT} measured by using FT (4) was more accurate than N_Γ calculated from the friction drag coefficient by using Eqs. (1) and (2) when the rotations occurred near the glass surface. Further, FT (4) may be applied to, e.g., bacterial flagella, linear motor proteins such as kinesins and myosins, and the transportations of vesicles and organelles in a cell. Because it is not easy to estimate friction drag coefficients in a cell, a nondestructive force measurement method such as FT (4) will be in demand in the future.

Methods.—The $\alpha_3\beta_3\gamma$ subcomplex [α(His$_6$/C193S)$_3\beta$(His$_{10}$)$_3\gamma$S107C/I210C] of F_1-ATPase from thermophilic *Bacillus* PS3 (called the wild-type F_1), the slow ATP cleavage $\alpha_3\beta_3\gamma$ subcomplex [α(His$_6$/C193S)$_3\beta$(His$_{10}$/E190D)$_3\gamma$S107C/I210C] (called the mutant F_1), and the V_1 complex from *Thermus thermophilus* were expressed in *E. coli*, purified and biotinylated [18,26]. As to the rotation assay, we used streptavidin-coated magnetic beads (200–700 nm, Seradyn) which are useful when F_1 is operated by magnetic tweezers or streptavidin-coated polystyrene beads. The magnetic beads were pulverized by using the ultrasonic bath sonicator to make them smaller. The rotary motion of F_1 (or V_1) was observed immobilizing the $\alpha_3\beta_3$ ring on a Ni-NTA glass surface (see *Material and Methods* in [23] for detail).

We thank members of our laboratory for discussions and technical advice. We thank Dr. H. Takagi for discussions on Eq. (4); and Dr. K. Yokoyama, Dr. H. Imamura, Dr. M. Nakano, and Y. Apa Nishikawa for discussions and providing samples, related to V_1. This work was supported by a JSPS Grant-in-aid (to K. H.), and Grants-in-aids for Scientific Research from MEXT (18074005 and 18201025 to H. N. and 21107517 (to R. I.), and a grant (to H. N.) from the Post-Silicon Alliance, ISIR at Osaka University.

*hnoji@sanken.osaka-u.ac.jp

[1] D. J. Evans, E. G. D. Cohen, and G. P. Morriss, Phys. Rev. Lett. **71**, 2401 (1993).
[2] G. E. Crooks, Phys. Rev. E **61**, 2361 (2000).
[3] C. Jarzynski, Phys. Rev. Lett. **78**, 2690 (1997).
[4] T. Harada and S. I. Sasa, Phys. Rev. Lett. **95**, 130602 (2005).
[5] G. M. Wang, E. M. Sevick, E. Mittag, D. J. Searles, and D. J. Evans, Phys. Rev. Lett. **89**, 050601 (2002).
[6] K. Feitosa and N. Menon, Phys. Rev. Lett. **92**, 164301 (2004).
[7] S. Ciliberto *et al.*, Physica A (Amsterdam) **340**, 240 (2004).
[8] K. Hayashi and H. Takagi, J. Phys. Soc. Jpn. **76**, 105001 (2007).
[9] J. Liphardt *et al.*, Science **296**, 1832 (2002).
[10] D. Collin *et al.*, Nature (London) **437**, 231 (2005).
[11] D. Mizuno, C. Tardin, C. F. Schmidt, and F. C. MacKintosh, Science **315**, 370 (2007).
[12] G. Muhmud *et al.*, Nature Phys. **5**, 606 (2009).
[13] H. Noji, R. Yasuda, M. Yoshida, and K. Kinosita, Jr., Nature (London) **386**, 299 (1997).
[14] R. Yasuda, H. Noji, K. Kinosita, Jr., and M. Yoshida, Cell **93**, 1117 (1998).
[15] H. Wang and G. Oster, Nature (London) **396**, 279 (1998).
[16] T. Masaike *et al.*, Nat. Struct. Mol. Biol. **15**, 1326 (2008).
[17] R. Yasuda *et al.*, Nature (London) **410**, 898 (2001).
[18] H. Noji *et al.*, J. Biol. Chem. **276**, 25480 (2001).
[19] N. Sakaki *et al.*, Biophys. J. **88**, 2047 (2005).
[20] O. Panke *et al.*, Biophys. J. **81**, 1220 (2001).
[21] Y. Sowa and R. M. Berry, Q. Rev. Biophys. **41**, 103 (2008).
[22] Y. Harada *et al.*, Nature (London) **409**, 113 (2001).
[23] See supplementary material at http://link.aps.org/supplemental/10.1103/PhysRevLett.104.218103 for details of our study.
[24] H. Ueno *et al.*, Biophys. J. (to be published).
[25] K. Shimabukuro *et al.*, Proc. Natl. Acad. Sci. U.S.A. **100**, 14731 (2003).
[26] H. Imamura *et al.*, Proc. Natl. Acad. Sci. U.S.A. **102**, 17929 (2005).